

# Forecast reconciliation for vaccine supply chain optimization

Bhanu Angam<sup>a</sup>, Alessandro Beretta<sup>b</sup>, Eli De Poorter<sup>a</sup>, Matthieu Duvinage<sup>b</sup> and Daniel Peralta<sup>a,\*</sup>

<sup>a</sup>IDLab, Department of Information Technology, Ghent University - imec, Technologiepark 126, 9052 Gent, Belgium

<sup>b</sup>GSK, Avenue Fleming, 20, 1300 Wavre - Belgium  
ORCID ID: Eli De Poorter <https://orcid.org/0000-0002-0214-5751>,  
Daniel Peralta <https://orcid.org/0000-0002-7544-8411>

**Abstract.** Vaccine supply chain optimization can benefit from hierarchical time series forecasting, when grouping the vaccines by type or location. However, forecasts of different hierarchy levels become incoherent when higher levels do not match the sum of the lower levels forecasts, which can be addressed by reconciliation methods.

In this paper, we tackle the vaccine sale forecasting problem by modeling sales data from GSK between 2010 and 2021 as a hierarchical time series. After forecasting future values with several ARIMA models, we systematically compare the performance of various reconciliation methods, using statistical tests. We also compare the performance of the forecast before and after COVID. The results highlight Minimum Trace and Weighted Least Squares with Structural scaling as the best performing methods, which provided a coherent forecast while reducing the forecast error of the baseline ARIMA.

## 1 Introduction

Forecasting vaccine demand is critical to practitioners; its underestimation lead to loss of customers and profits, whereas its overestimation would cause the expiry of produced vaccines and a waste of resources [2, 10]. Vaccine demand forecasting is mostly done by replicating values from previous years [15, 7], sometimes combining them with demographic information [9]. However, machine learning techniques become necessary to obtain better solutions to this problem.

Given enough previous data, vaccine demand can be modeled as a time series, that is, a sequence of values measured in fixed time intervals [13]. There are various methods to forecast future values in a time series. Among them, linear methods like ARIMA are still widely used, due to their interpretability and stability. In many domains, time series can be arranged in the form of a hierarchy [14]. For instance, sales can be split into geographical regions or product types, where the series at one level corresponds to the sum of the values of the series at the immediately lower level. Each of these time series can be independently forecast; however, the coherency of the time series is lost: the forecast of a higher level does not correspond to the sum of the forecasts of lower levels.

Forecast combination methods ensure the coherency of the forecasts by only forecasting the series at one level (typically the highest

or the lowest), and then calculating the forecasts for the rest of the hierarchy [11, 12]. Their main limitation is that they use only one level of the hierarchy to compute the forecasts. Forecasting reconciliation aims at obtaining coherent forecasts based on the entire hierarchy [12, 13, 1]. Several methods have been proposed in the field, such as Ordinary Least Squares [14], Weighted Least Squares [13] and Trace Minimization [17]. Frequently, the values of the time series are limited to a certain range, which is often the positive real or integer numbers. Positive outcomes when forecasting are usually enforced by taking the logarithm of the series; however, when applying the reconciliation in the original space it is possible that some forecasts become negative. Therefore, some methods have been proposed to enforce positive reconciled forecasts [18].

There are a few works in the scientific literature that model vaccine demand as a time series and then forecast future values. In [16], ARIMA was applied to forecast vaccine demand in Indonesia. In [4], a cloud infrastructure used a Long Short-Term Memory (LSTM) to forecast the demand for COVID-19 vaccines. However, none of these works consider hierarchical time series to forecast vaccine demand.

In this paper, we compare several state-of-the-art combination and reconciliation methods to adjust the ARIMA forecast of the vaccine sales of a hierarchy of products across several geographical areas. We also evaluate the impact of COVID-19 on the sales, analyzing how the forecast error increases after COVID-19 due to large unexpected changes in demand patterns. We carry out a series of statistical tests on the obtained results, and come to the conclusion that, for this dataset, Minimum Trace and Weighted Least Squares with Structural scaling were the best performing reconciliation methods, achieving reconciled forecasts while also lowering the forecast error.

The main contributions of this paper are the following:

- Comparison of various combination and reconciliation methods for adjusting the ARIMA forecast of vaccine sales in a hierarchical product structure.
- Evaluation of the impact of COVID-19 on sales and demonstrating an increase in forecast error due to changes in demand patterns.
- Finally, through statistical tests, we conclude that Minimum Trace and Weighted Least Squares with Structural scaling are the best performing and most robust reconciliation methods for the dataset used.

\* Corresponding Author. Email: [daniel.peralta@ugent.be](mailto:daniel.peralta@ugent.be).

This paper is structured as follows. First, Section 2 introduces the topic of forecast recombination and reconciliation in hierarchical time series. Section 3 describes the methodology carried out in this study, including the dataset analyzed and its preprocessing. The results of the experiments are presented and analyzed in Section 4. Finally, Section 5 presents the conclusions of this study.

## 2 Background

### 2.1 Hierarchical time series

In a hierarchical time series, the values of a particular level can be expressed as the sum of values at the immediately lower level. A hierarchical time series with  $n$  observations,  $k$  levels, a total of  $m$  series, and  $m_i$  series in level  $i$  can be expressed as a matrix  $\mathbf{Y}_t$  with dimensions  $m \times n$ , where each row contains one of the time series. Therefore, the hierarchical time series can be expressed as  $\mathbf{Y}_t = \mathbf{S}\mathbf{Y}_{k,t}$ , where  $\mathbf{S}$  is a summing matrix with dimensions  $m \times m_k$  and  $\mathbf{Y}_{k,t}$  contains the series at the bottom level of the hierarchy. The example hierarchy shown in Fig. 1 can be represented as (1). Note that the bottom  $m_k$  rows of  $\mathbf{S}$  are the identity matrix  $\mathbf{I}_{m_k}$ .

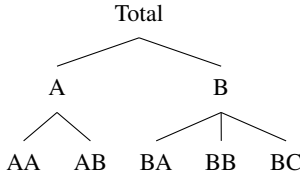


Figure 1: Example of a simple hierarchy

$$\begin{bmatrix} Y_{T,t} \\ Y_{A,t} \\ Y_{B,t} \\ Y_{AA,t} \\ Y_{AB,t} \\ Y_{BA,t} \\ Y_{BB,t} \\ Y_{BC,t} \end{bmatrix} = \begin{bmatrix} 1 & 1 & 1 & 1 & 1 \\ 1 & 1 & 0 & 0 & 0 \\ 0 & 0 & 1 & 1 & 1 \\ 1 & 0 & 0 & 0 & 0 \\ 0 & 1 & 0 & 0 & 0 \\ 0 & 0 & 1 & 0 & 0 \\ 0 & 0 & 0 & 1 & 0 \\ 0 & 0 & 0 & 0 & 1 \end{bmatrix} \begin{bmatrix} Y_{AA,t} \\ Y_{AB,t} \\ Y_{BA,t} \\ Y_{BB,t} \\ Y_{BC,t} \end{bmatrix}. \quad (1)$$

In general, given  $h$ -step-ahead independent forecasts for the base series  $\hat{\mathbf{Y}}_n(h)$ , a final forecast  $\tilde{\mathbf{Y}}_n(h)$  can be estimated for all series as shown in (2), where  $\mathbf{G}$  is an  $m_k \times m$  matrix.

$$\tilde{\mathbf{Y}}_n(h) = \mathbf{S}\mathbf{G}\hat{\mathbf{Y}}_n(h) \quad (2)$$

### 2.2 Forecast combination

Forecast combination methods [5] typically forecast the time series of one hierarchy level, and extrapolate the forecasts via aggregation or proportion. In this way, the coherence of the forecasts is guaranteed.

#### 2.2.1 Bottom-up (BU)

It is arguably the simplest hierarchical forecast method, consisting of forecasting only the base level of the hierarchy, and then aggregating the forecasts using  $\mathbf{S}$  for the rest of the hierarchy. The matrix  $\mathbf{G}$  is defined as shown in (3), which yields  $\mathbf{S}\mathbf{G}_{BU} = \mathbf{S}$ .

$$\mathbf{G}_{BU} = [\mathbf{0}_{m_k \times (m-m_k)} \quad \mathbf{I}_{m_k}] \quad (3)$$

#### 2.2.2 Top-down (TD)

It computes forecasts only for the top level of the hierarchy, and then splits the values across all hierarchical levels using factors, which are estimated from previous values of the series. Typically, the proportions of historical averages  $\mathbf{p}$  are used [3, 1], as shown in (4), in combination with matrix  $\mathbf{G}$  (5). A drawback of this approach is that the forecasts are biased, for any  $\mathbf{p}$ , even if the base forecasts are unbiased [14].

$$p_j = \frac{\sum_{t=1}^n Y_{j,t}}{\sum_{t=1}^n Y_t}, \quad j = 1, \dots, m_k \quad (4)$$

$$\mathbf{G}_{TD} = [\mathbf{p} \quad \mathbf{0}_{m_k \times (m-1)}] \quad (5)$$

### 2.3 Forecast reconciliation

Forecast reconciliation methods, although sometimes categorized as combination methods, have the particularity that a forecast is computed for every individual time series in the hierarchy, and these forecasts are then adjusted to increase their coherence.

#### 2.3.1 Generalized Least Squares (GLS)

The base forecasts can be rewritten as in (6), where  $\beta_n(h)$  is the unknown mean of the future values of the bottom level of the hierarchy, and  $\epsilon_n$  has zero mean and covariance matrix  $\Sigma_n$ . Additionally, Hyndman et al. [14] demonstrated that adjusted forecasts (following (2)) are unbiased if and only if constraint (7) is met.

$$\hat{\mathbf{Y}}_n(h) = \mathbf{S}\beta_n(h) + \epsilon_n \quad (6)$$

$$\beta_n(h) = E[\mathbf{Y}_{k,n+h} | \mathbf{Y}_1, \dots, \mathbf{Y}_{m_k}]$$

$$\mathbf{G}\mathbf{S} = \mathbf{S} \quad (7)$$

Combining these definitions, an unbiased estimate for  $\beta_n(h)$  can be obtained by GLS estimation as in (8), where  $\Sigma_h^\dagger$  is the Moore-Penrose pseudoinverse of  $\Sigma_h$ . The main difficulty with this formulation is that estimating  $\Sigma_h$  and subsequently computing  $\Sigma_h^\dagger$  can be difficult for large hierarchies. The different reconciliation methods described in the next few subsections use different estimates for  $\Sigma_h$ .

$$\hat{\beta}_n(h) = (\mathbf{S}'\Sigma_h^\dagger\mathbf{S})^{-1}\mathbf{S}'\Sigma_h^\dagger\hat{\mathbf{Y}}_n(h)$$

$$\tilde{\mathbf{Y}}_n(h) = \mathbf{S}\hat{\beta}_n(h) = \mathbf{S}\mathbf{G}_{GLS}\hat{\mathbf{Y}}_n(h) \quad (8)$$

$$\mathbf{G}_{GLS} = (\mathbf{S}'\Sigma_h^\dagger\mathbf{S})^{-1}\mathbf{S}'\Sigma_h^\dagger$$

#### 2.3.2 Ordinary Least Squares (OLS)

By assuming that the errors are aggregated across the hierarchy in the same way as the series themselves ( $\epsilon_h \approx \mathbf{S}\epsilon_{k,h}$ ), OLS can be applied and  $\mathbf{G}$  can be derived as shown in (9) [14]. Interestingly, this optimal value for  $\mathbf{G}$  depends exclusively on the summing matrix and not on the data itself.

$$\mathbf{G}_{OLS} = \mathbf{S}(\mathbf{S}'\mathbf{S})^{-1}\mathbf{S}' \quad (9)$$

### 2.3.3 Minimum Trace (MinT)

Wickramasuriya et al. [17] showed that the covariance matrix of the coherent forecast errors follows (10), where  $\mathbf{W}_h$  is the covariance matrix of the base forecast errors. In this setting, we want to find the  $\mathbf{G}$  that minimizes the error variances, whose sum is the trace of  $\mathbf{V}_h$ , while respecting the constraint for an unbiased forecast in (7), as shown in (11).

$$\begin{aligned}\mathbf{V}_h &= \text{Var} \left[ \mathbf{Y}_{n+h} - \tilde{\mathbf{Y}}_n(h) \right] = \mathbf{S}\mathbf{G}\mathbf{W}_h\mathbf{G}'\mathbf{S}' \\ \mathbf{W}_h &= \text{Var} \left[ \mathbf{Y}_{n+h} - \hat{\mathbf{Y}}_n(h) \right]\end{aligned}\quad (10)$$

$$\begin{aligned}\mathbf{G}_{MinT} &= (\mathbf{S}'\mathbf{W}_h^{-1}\mathbf{S})^{-1}\mathbf{S}'\mathbf{W}_h^{-1} \\ \tilde{\mathbf{Y}}_n(h) &= \mathbf{S}(\mathbf{S}'\mathbf{W}_h^{-1}\mathbf{S})^{-1}\mathbf{S}'\mathbf{W}_h^{-1}\hat{\mathbf{Y}}_n(h)\end{aligned}\quad (11)$$

Naturally,  $\mathbf{W}_h$  is unknown and has to be estimated from the training data; different estimates yield different reconciliation methods. Note that assuming that  $\mathbf{G}$  is independent of the data—and therefore  $\mathbf{W}_h = \mathbf{I}_m$ —yields OLS. Also, note that the estimates of  $\mathbf{W}_h$  usually include a scaling factor in the original publications [17, 13], which is only relevant when computing confidence intervals and is canceled out when applying (11). For the sake of simplicity, in this paper we assume that the constant is 1.

Equation (12) shows a more relaxed assumption: that the error covariance matrices are proportional to each other. This allows us to estimate the matrix for  $h = 1$ , and derive  $\mathbf{W}_h$  from it. In this case,  $\mathbf{W}_1$  is estimated based on the sample covariance of the residuals. Throughout this paper, this is the method we will refer to as *MinT*.

$$\mathbf{W}_h = \mathbf{W}_1 \quad (12)$$

### 2.3.4 Weighted Least Squares with Variance scaling (WLSV)

When  $\mathbf{W}_h$  is defined as in (13), where  $\mathbf{e}_t$  is an  $m$ -dimensional vector containing the residuals of the base models trained on each series, the weights for each series are scaled according to the variance of the residuals of the base forecasts.

$$\begin{aligned}\mathbf{W}_h &= \text{diag}(\hat{\mathbf{W}}_1) \\ \hat{\mathbf{W}}_1 &= \frac{1}{T} \sum_{t=1}^T \mathbf{e}_t \mathbf{e}_t'\end{aligned}\quad (13)$$

### 2.3.5 Weighted Least Squares with Structural scaling (WLSS)

In this case, we define  $\mathbf{W}_h$  as in Equation 14. In other words, each value along the diagonal of  $\mathbf{W}_h$  corresponds to the sum of the corresponding row in  $\mathbf{S}$ , which makes it dependent exclusively on the structure of the hierarchy and not on the values of the time series nor the models.

$$\mathbf{W}_h = \text{diag}(\mathbf{S}\mathbf{1}_{m_k}) \quad (14)$$

### 2.3.6 Non-negative reconciliation (NNOLS and NNMinT)

Previously described methods do not ensure that the reconciled forecasts are non-negative, which is a constraint in many real-life problems. In fact, a sufficient condition for the non-negativity of  $\tilde{\mathbf{Y}}_n(h)$  is that vectors  $\tilde{\mathbf{b}}_n(h) = \mathbf{G}\hat{\mathbf{Y}}_n(h)$  should be non-negative, as can be derived from (2). In [18], it is demonstrated that this the optimal  $\tilde{\mathbf{b}}_n(h)$  is the solution of the quadratic programming problem in (15).

$$\begin{aligned}\tilde{\mathbf{b}}_n(h) &= \min_{\tilde{\mathbf{b}}} \frac{1}{2} \tilde{\mathbf{b}}' \mathbf{S}' \mathbf{W}_h^{-1} \mathbf{S} \tilde{\mathbf{b}} - \tilde{\mathbf{b}}' \mathbf{S}' \mathbf{W}_h^{-1} \hat{\mathbf{Y}}_n(h) \\ \text{s.t. } &\tilde{b}_i \geq 0 \quad \forall i \in \{1, \dots, m\}\end{aligned}\quad (15)$$

## 3 Forecast reconciliation of vaccine sales

In this paper, we applied classic and state of the art methods to reconcile vaccine sales hierarchical time series. Section 3.1 describes the dataset tackled. Then, Section 3.2 describes the preprocessing applied on the dataset, Section 3.3 depicts the combination and reconciliation methods that were considered in this study, and Section 3.4 describes the model selection procedure followed to choose the hyperparameters for the forecast.

### 3.1 Dataset

The dataset used for this study consists of monthly vaccine sales from GSK, between years 2010 and 2021. The time series hierarchy has 5 levels: commercial segment, product family, aggregated product, product type and stock keeping unit. To ensure that the lowest level time series contain sufficient data, we focus on the top 3 levels of the hierarchy (noted as CS, PF and AP respectively), which are composed by 3, 10 and 16 time series, respectively, as shown in Fig. 2. It is noteworthy that some series start later than 2010, typically because they refer to recently developed products.

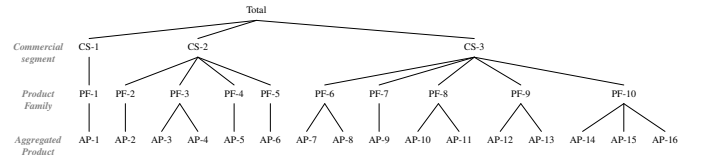


Figure 2: Hierarchical representation of the dataset

Because the time series represent sales numbers, their values are, in general, non-negative integers. However, the raw time series collected directly from the sales department also contains corrections done at the end of the year to compensate for registration errors and ensure that yearly totals are correct. This causes some of the time series values to have unexpectedly large or small values, leading to negative values and breaking seasonal patterns, which in turns adds to the complexity of the problem.

The data was split into training and forecast periods. Due to a potentially different behavior of the time series during the COVID-19 pandemic, two different splits were considered, which either excluded the pandemic period from the data, or included it entirely in the forecast period, as shown in Table 1.

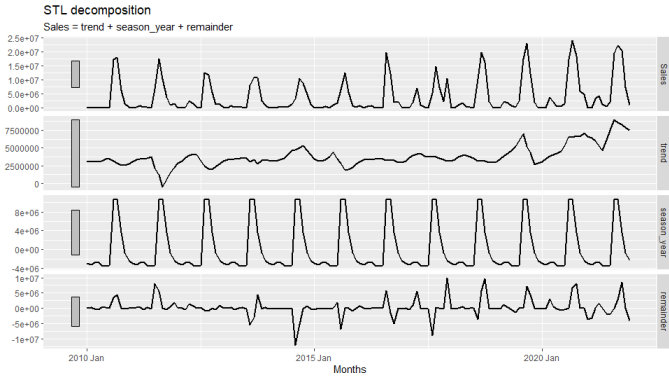
**Table 1:** Train and forecast period splits of data.

Period	Before COVID-19	After COVID-19
Train period	2010 - 2017	2010 - 2019
Forecast period	2018 - 2019	2020 - 2021

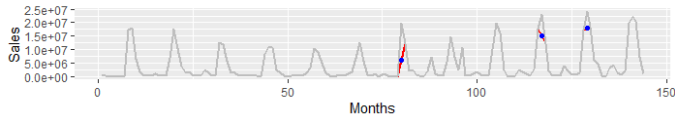
### 3.2 Preprocessing

Negative values in the time series were replaced by a linear interpolation of the preceding and following values, while shifting all the values for that year proportionally, to ensure that the total sales volume for the year remains the same. This was done at the PF level of the hierarchy.

The outlier detection was carried out by first applying a Seasonal and Trend decomposition using Loess decomposition (STL) [8], to extract seasonal, trend and remainder components from the series. Then, values in the remainder that deviate from the quartiles by more than 3 times the inter-quartile range were considered to be outliers, following other works in the field [13]. As an example, Fig. 3 shows the STL decomposition and the corrected outliers of time series PF3, which is clearly seasonal.



(a) STL decomposition of PF3. Outlier detection is made on the remainder component.



(b) Detected outliers from the remainder of above decomposition are replaced by linear interpolation. The blue dot is the replacement for the outlier, and the red line is the smoothed curve.

**Figure 3:** STL decomposition and outlier detection on the remainder.

### 3.3 Forecasting

The entire pipeline applied on this problem is shown on Fig. 4.

The time series were normalized with a Box-Cox transformation (Equation 16), with  $\lambda$  being estimated using profile likelihood function and goodness of fit tests for normality, and where  $\lambda_2 = \min y_i$ .

$$y_i^{(\lambda)} = \begin{cases} \frac{(y_i + \lambda_2)^\lambda - 1}{\lambda} & \text{if } \lambda \neq 0 \\ \ln(y_i + \lambda_2) & \text{if } \lambda = 0 \end{cases} \quad (16)$$

After normalization, we train a seasonal ARIMA model for each time series in the hierarchy. Naturally, each of these time series

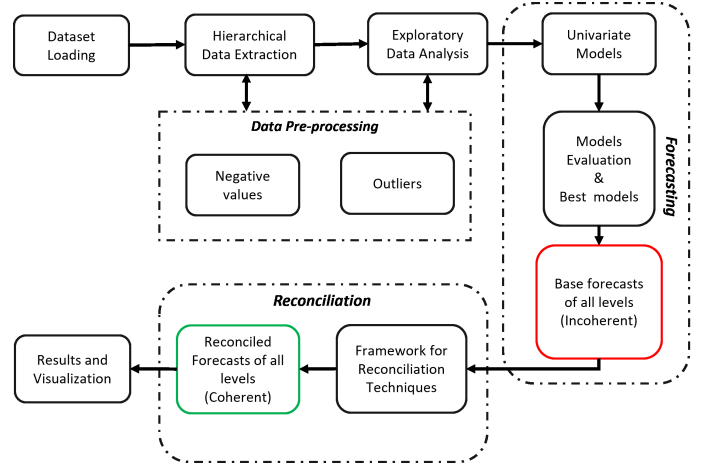


**Figure 4:** General workflow of the proposal.

might have a different seasonality and dependencies on lagged values; therefore, a model selection has to be done when training each series.

### 3.4 Model selection

To compute the baseline forecasts of the time series, Seasonal ARIMA [13] models were trained with 4 different parameters for the seasonality (1, 3, 6 and 12) months. Additionally, the non-seasonal ( $p$ ,  $d$  and  $q$ ) and seasonal ( $P$ ,  $D$  and  $Q$ ) parameters of ARIMA must be chosen. The differencing term  $d$  was estimated using two tests—Kwiatkowski, Phillips, Schmidt–Shin (KPSS) and Dickey–Fuller (ADF)—and taking the maximum value from both. The seasonal differencing  $D$  was estimated by Osborn, Chui, Smith, and Birchenhall (OCSB) test. The remaining parameters were estimated via a grid search within the training set, using Akaike’s Information Criterion (AIC) as the optimized metric.

After the 6 hyperparameters for each seasonality have been optimized, we must select the seasonal frequency that obtains the best results. This is done by choosing the one that yields the best symmetric mean absolute percentage error (SMAPE). To this purpose, a specific variant of cross-validation is applied (rolling forecasting origin [6]), where the size of the training set is increased for each iteration, and the validation set has a fixed size and always starts immediately after the training set (Fig. 5).

The rolling forecasting origin was performed with a minimum training set size of 28 months, and a validation set size of 2 months, increasing the size of the training set 1 month at a time. As there are a total of 84 months in the entire training set, this yielded 54 pairs of training and validation sets.



**Figure 5:** Cross-validation by rolling origin (training set in green, validation set in red)

### 3.5 Reconciliation

After computing the forecast for all time series, we reconcile the forecasts using the methods described in Section 2.3, namely BU, OLS, NNOLS, WLSS, WLSV and MINT.

### 3.6 Performance measures

Two performance measures were used to evaluate the forecasts and their reconciliations:

**Sales Forecast Bias (SFB)** measures the tendencies to over- and underforecast along a certain period of length  $T$ , rather than at individual points in time. This measure is often used by companies to evaluate sales predictions, because an over-estimation in a certain month can be compensated by an equivalent under-estimation in the following month (or vice-versa). The SFB of a certain time series  $i$  is computed as shown in Equation 17.

$$SFB_i = \frac{\sum_{s=1}^T [\hat{Y}_{i,n-s}(h) - Y_{i,n-s}(h)]}{\sum_{s=1}^T Y_{i,n-s}(h)} \times 100 \quad (17)$$

In this work, we calculated the SFB as a percentage over a period of 6 months ( $T = 6$ ). To aggregate results for multiple time series while avoiding the cancellation of positive and negative errors, we computed the weighted average of the absolute values of SFB for all series (volume-Weighted SFB, WSFB, Equation 18), where the weight  $w_i$  is the sum of all values of a time series:

$$WSFB = \frac{\sum_{i=1}^m w_i SFB_i}{\sum_{i=1}^m w_i} \quad (18)$$

$$w_i = \sum Y_{i,t}$$

**Root mean squared scaled error (RMSSE)** is an error measure scaled by the difference between consecutive values in the series as shown in Equation 19.

$$RMSSE = \sqrt{\frac{\frac{1}{h} \sum_{t=n+1}^{n+h} (y_t - \hat{y}_t)^2}{\frac{1}{n-1} \sum_{t=2}^n (y_t - y_{t-1})^2}} \quad (19)$$

Similarly to the SFB in Equation 18, we compute the weighted average of the RMSSE when aggregating over multiple time series.

## 4 Results

This section describes the results obtained from the experiments. First, baseline results are presented in Section 4.1. The results of the different reconciliation methods are shown in Section 4.2. Section 4.3 compares the behavior of the results, and finally Section 4.4 presents a general discussion of the results.

### 4.1 Baseline forecasting

Table 2 and Fig. 6 present an overview of the SFB and RMSSE obtained using the baseline forecast method for each series, at each level of the hierarchy. As expected, it can clearly be seen that the highest level in the hierarchy (Commercial segment) is easier to predict than lower levels, whose series are subject to a higher variability. However, the difference in forecast error between the two lowest levels is very small, and the range of obtained errors differs greatly. Some series are very accurately predicted, while others have a large forecast error. The plots also reflect an increase in the errors after COVID-19.

**Table 2:** Baseline ARIMA results for each hierarchical level

Level	Series	SFB		RMSSE	
		Before COVID	After COVID	Before COVID	After COVID
Commercial segment	CS1	0.0823	0.0970	0.8500	0.8101
	CS2	0.1040	0.1530	0.2975	0.6108
	CS3	0.1174	0.2020	1.2340	1.8258
Product family	PF1	0.1200	0.1330	1.2514	1.2734
	PF2	0.1400	0.0790	0.9094	0.8255
	PF3	0.2200	0.2710	1.7796	2.5599
	PF4	0.0870	0.2550	0.8804	2.1496
	PF5	0.2300	0.2540	3.2135	2.7705
	PF6	0.2700	0.1210	1.1544	1.5091
	PF7	0.2890	0.3460	0.5860	0.7630
	PF8	0.1110	0.0970	0.4999	0.8568
	PF9	0.1300	0.1870	2.3414	2.4231
	PF10	0.2400	0.2820	2.6340	3.7584
Aggregated product	AP1	0.0860	0.1810	1.7226	2.4580
	AP2	0.1020	0.0410	0.8710	0.8318
	AP3	0.1940	0.1710	0.7796	1.1590
	AP4	0.1870	0.2910	2.5067	3.0681
	AP5	0.2960	0.2760	3.2135	3.0005
	AP6	0.1210	0.1010	0.6460	0.8516
	AP7	0.1290	0.3980	1.1353	1.2203
	AP8	0.1830	0.0210	1.1544	2.5091
	AP9	0.3670	0.4120	1.1474	2.9291
	AP10	0.2440	0.4630	0.4702	1.8843
	AP11	0.0750	0.1000	1.1219	1.9539
	AP12	0.0710	0.0970	0.4999	1.8357
	AP13	0.3990	0.3830	1.8604	1.5216
	AP14	0.2320	0.2420	1.9526	2.3568
	AP15	0.1460	0.2820	3.2340	3.3258
	AP16	0.2500	0.3780	1.1624	1.7590

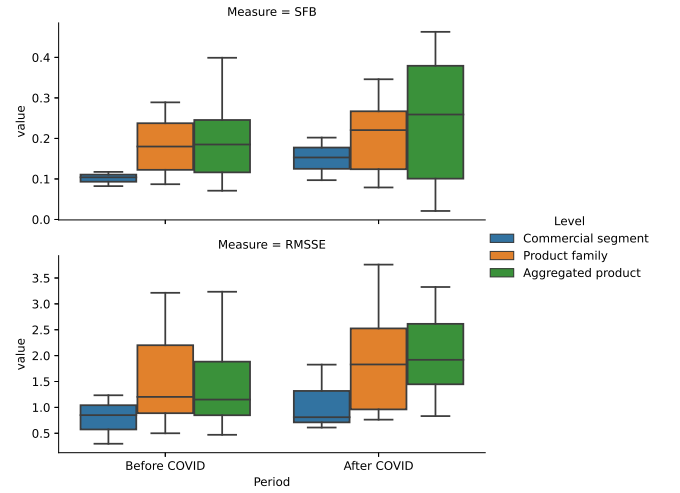


**Figure 6:** Distribution of baseline results

### 4.2 Reconciliation

Figure 7 shows the SFB and RMSSE obtained for all time series and reconciliation methods. As was observed in the previous section, we can see that the highest level of the hierarchy is easier to predict than the two lowest levels, a behavior that is consistent across all methods tested.

Although all methods seem to improve on the baseline, MINT and WLSS obtain the lowest SRB and RMSSE in the two tested periods and for all hierarchy levels. However, the boxplots show a large overlap of the error values, which makes it difficult to conclude whether the results of all individual time series are consistently improved by these methods. Figure 8 shows the difference in SFB and RMSSE obtained by each method with respect to the result obtained by the baseline. We also see that most differences are indeed negative, indicating that in a vast majority of the cases the results of the baseline are improved. As expected, the combination method BU doesn't modify the forecast for the base level of the hierarchy. WLSS and MINT improve the results almost in all cases.

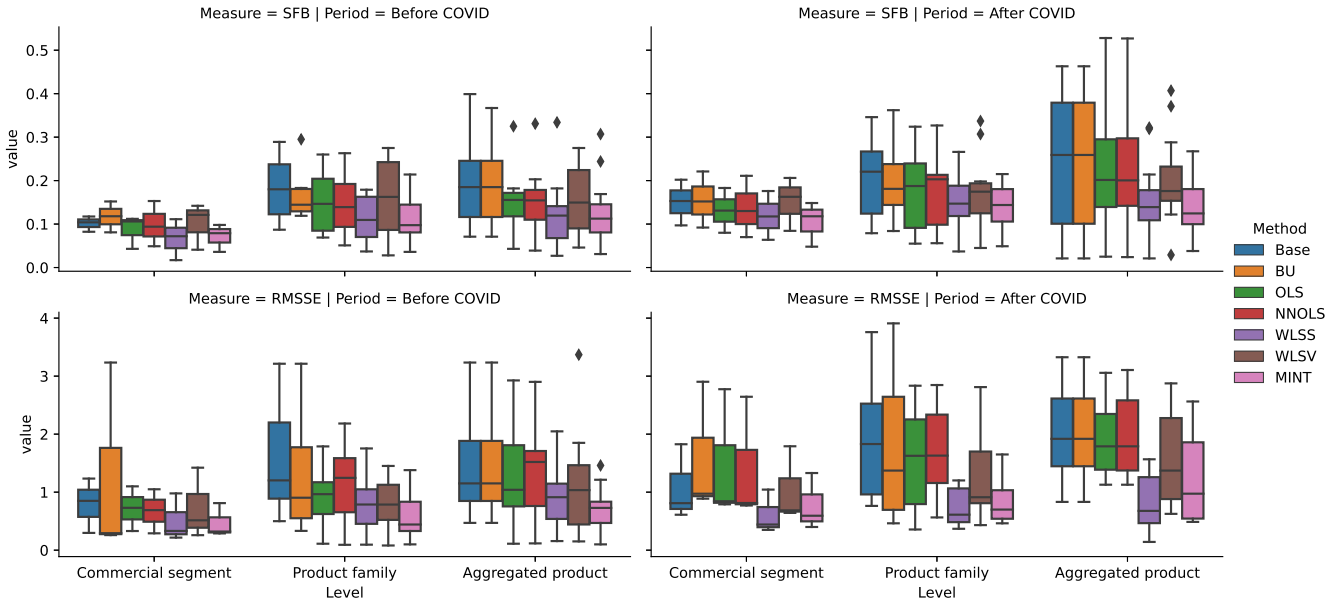


Figure 7: Distribution of results after reconciliation

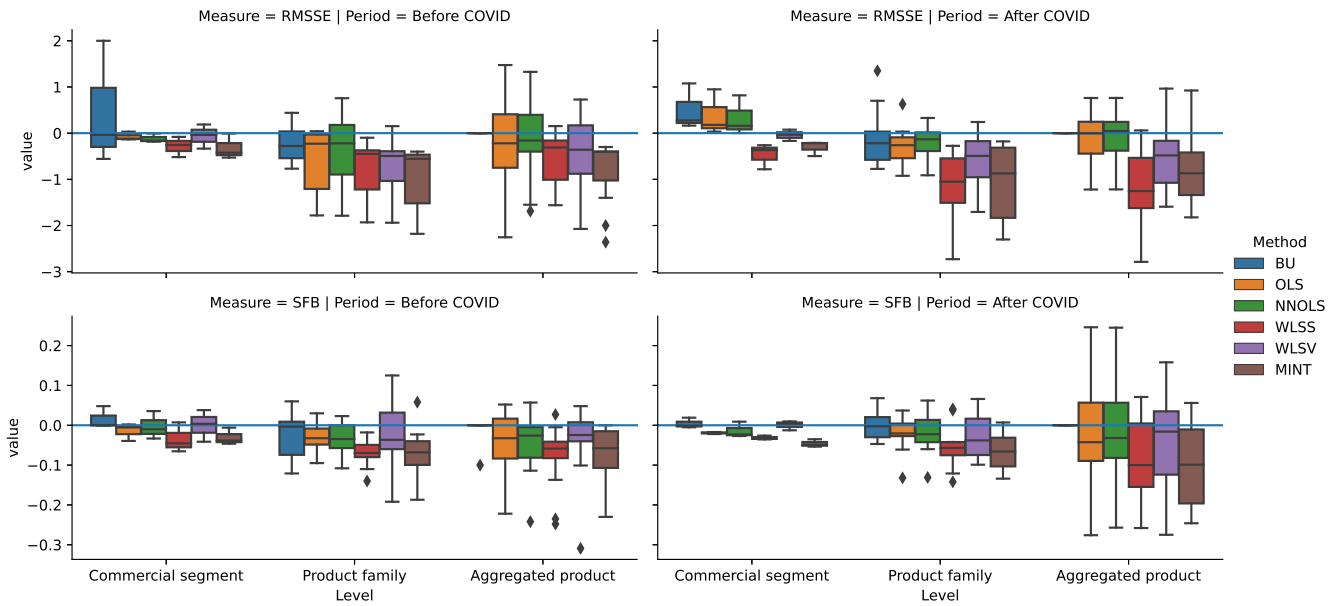


Figure 8: Distribution of the differences with respect to base forecast.

For reference, the complete results are reported in the Tables 6 and 7.

### 4.3 Comparison before/after COVID-19

In the previous figures, it could be seen that, in general, the error increased in the period after COVID-19. As initially expected, forecasting the behavior of the series after the start COVID-19 is more difficult, as the test data differs more from the training data. This trend is observed for all methods and levels, but is more accused in the lowest level of the hierarchy, where we can see that some forecasts achieve very large errors, and also that, for some of the series, the reconciliation methods produce forecasts that are worse than the

baseline. Only WLSS and MINT seem to escape this trend, having the 75th percentile of the difference in SFB and RMSSE (Fig. 8) below zero for both measures and for all hierarchy levels, indicating that at least 75% of the time series have their forecast improved by these reconciliation methods.

### 4.4 Discussion

In this section, we carry out a statistical analysis of the results obtained in this experimental study, in order to determine if the differences observed in the results of the different methods are statistically significant or not. First, Table 3 shows the results of the Friedman

test to determine whether there is any difference in the distributions of the SFB and RMSSE values obtained by all methods.

**Table 3:** Results of Friedman test

	Statistic	p-value
SFB	108.1	5.081e-21
RMSSE	164.2	7.504e-33

Clearly, there are differences in the distributions, which enables us to apply a Dunn test to evaluate potential differences in the results of every combination and reconciliation method, using the baseline as a reference in every case. Holm’s method was applied for p-value adjustment. The results of this test are shown in Table 4. In the table, we can see that WLSS and MINT obtain statistically significant differences with the baseline method. This result is in line with the previous observation that these two algorithms outperformed the rest systematically, for all aggregation levels, both before and after COVID.

To conclude the study, Table 5 shows the results of Wilcoxon’s test to compare the performance of all methods, at all levels, before and after COVID. Clearly, there is a statistically significant performance drop when test values after COVID are considered, despite the use of a larger training set, indicating an important change in the behavior of the time series analyzed.

**Table 4:** Results of Dunn test with Holm p-value adjustment

	SFB	RMSSE
Base	1	1
BU	1	1
OLS	1	1
NNOLS	1	1
WLSS	0.004067	1.012e-06
WLSV	1	0.06092
MINT	0.001384	1.53e-06

**Table 5:** Results of Wilcoxon’s test with Bonferroni correction

	Statistic	p-value
SFB	4546	9.988e-11
RMSSE	3488	5.116e-16

## 5 Conclusion

Vaccine demand prediction is a critical problem in industry, with a large impact on public health and economy. For the first time, we have modeled this problem as a hierarchical time series forecast, establishing a hierarchy based on product families and gathering sales data between 2010 and 2021 in GSK.

Then, we have carried out a comparison of the results of different forecast reconciliation methods for hierarchical time series, applied on a real dataset of vaccine sales containing a 3-level hierarchy over 12 years. The baseline forecast for each level of the hierarchy was computed with ARIMA, and results were computed in a rolled cross-validation scheme.

The analysis has shown that MINT and WLSS obtained the best results for the forecast, a conclusion that is supported by statistical significance of the performed tests, while producing forecasts that are reconciled along the entire hierarchy. Furthermore, we have observed that the algorithms systematically obtain worse forecasts when data during the COVID period is used as test set, despite the use of more

years of training data. This indicates a significant change of the behavior of the time series during this period. However, MINT and WLSS are again able to yield better results than the rest of the methods analyzed, palliating the performance drop, indicating their higher robustness to this kind of changes.

## Acknowledgements

This work was sponsored by GlaxoSmithKline Biologicals SA.

## Author contributions

AB, BA, DP, MD were involved in the conception and design of the study and/or the development of the study protocol. AB, BA participated to the acquisition of data. AB, BA, DP, MD analysed and interpreted the results. All authors were involved in drafting the manuscript or revising it critically for important intellectual content. AB and BA had full access to the data. All authors approved the manuscript before it was submitted by the corresponding author.

## Conflict of interest

MD and AB are employees of the GSK group of companies.

## References

- [1] Mahdi Abolghasemi, Rob J. Hyndman, Evangelos Spiliotis, and Christoph Bergmeir, ‘Model selection in reconciling hierarchical time series’, *Machine Learning*, **111**, 739–789, (2 2022).
- [2] Jon Kim Andrus, Jacqueline Sherris, John W. Fitzsimmons, Mark A. Kane, and M. Teresa Aguado, ‘Introduction of human papillomavirus vaccines into developing countries - international strategies for funding and procurement’, *Vaccine*, **26**, K87–K92, (8 2008).
- [3] George Athanasopoulos, Puwasala Gamakumara, Anastasios Panagiotelis, Rob J. Hyndman, and Mohamed Affan, ‘Hierarchical forecasting’, *Advanced Studies in Theoretical and Applied Econometrics*, **52**, 689–719, (2020).
- [4] Miguel Barajas, Shilpa Bhatkande, Pireethi Baskaran, Hardik Gohel, and Bishwajeet Pandey, ‘Advancing deep learning for supply chain optimization of covid-19 vaccination in rural communities’, *Proceedings - 2021 IEEE 10th International Conference on Communication Systems and Network Technologies, CSNT 2021*, 690–695, (2021).
- [5] J. M. Bates and C. W. J. Granger, ‘The combination of forecasts’, *Journal of the Operational Research Society*, **20**, 451–468, (12 1969).
- [6] Christoph Bergmeir, Rob J. Hyndman, and Bonsoo Koo, ‘A note on the validity of cross-validation for evaluating autoregressive time series prediction’, *Computational Statistics and Data Analysis*, **120**, 70–83, (4 2018).
- [7] Tania Cernuschi, Stefano Malvoti, Emily Nickels, and Martin Friede, ‘Bacillus calmette-guérin (bcg) vaccine: A global assessment of demand and supply balance’, *Vaccine*, **36**, 498–506, (1 2018).
- [8] R. B. Cleveland, W. S. Cleveland, J. E. McRae, and I. J. Terpenning, ‘Stl: A seasonal-trend decomposition procedure based on loess’, *Journal of Official Statistics*, **6**, 3–73, (1990).
- [9] Frédéric Debellut, Nathaniel Hendrix, Virginia E. Pitzer, Kathleen M. Neuzil, Dagna Constenla, Naor Bar-Zeev, Anthony Marfin, and Clint Pecenka, ‘Forecasting demand for the typhoid conjugate vaccine in low- and middle-income countries’, *Clinical Infectious Diseases*, **68**, S154–S160, (3 2019).
- [10] Shawn A.N. Gilchrist and Angeline Nanni, ‘Lessons learned in shaping vaccine markets in low-income countries: a review of the vaccine market segment supported by the gavi alliance’, *Health Policy and Planning*, **28**, 838–846, (12 2013).
- [11] Charles W. Gross and Jeffrey E. Sohl, ‘Disaggregation methods to expedite product line forecasting’, *Journal of Forecasting*, **9**, 233–254, (5 1990).
- [12] Ross Hollyman, Fotios Petropoulos, and Michael E. Tipping, ‘Understanding forecast reconciliation’, *European Journal of Operational Research*, **294**, 149–160, (10 2021).

- [13] R.J. Hyndman and G. Athanasopoulos, *Forecasting: principles and practice*, OTexts, 3rd edition edn., 2021.
- [14] Rob J. Hyndman, Roman A. Ahmed, George Athanasopoulos, and Han Lin Shang, 'Optimal combination forecasts for hierarchical time series', *Computational Statistics and Data Analysis*, **55**, 2579–2589, (9 2011).
- [15] Leslie E. Mueller, Leila A. Haidari, Angela R. Wateska, Roslyn J. Phillips, Michelle M. Schmitz, Diana L. Connor, Bryan A. Norman, Shawn T. Brown, Joel S. Welling, and Bruce Y. Lee, 'The impact of implementing a demand forecasting system into a low-income country's supply chain', *Vaccine*, **34**, 3663–3669, (7 2016).
- [16] Julian Satya Sahisnu, Friska Natalia, Ferry Vincenttius Ferdinand, Sud Sudirman, and Chang Seong Ko, 'Vaccine prediction system using arima method', *ICIC Express Letters, Part B: Applications*, **11**, 567–575, (2020).
- [17] Shanika L. Wickramasuriya, George Athanasopoulos, and Rob J. Hyndman, 'Optimal forecast reconciliation for hierarchical and grouped time series through trace minimization', *Journal of the American Statistical Association*, **114**, 804–819, (4 2019).
- [18] Shanika L. Wickramasuriya, Berwin A. Turlach, and Rob J. Hyndman, 'Optimal non-negative forecast reconciliation', *Statistics and Computing*, **30**, 1167–1182, (9 2020).

## A Supplementary material: complete result tables

**Table 6:** SFB after reconciliation, for all levels and methods

Series	Before COVID							After COVID						
	Base	BU	OLS	NNOLS	WLS	WLSV	MINT	Base	BU	OLS	NNOLS	WLS	WLSV	MINT
CS1	.0823	.0810	.0430	.0490	.0170	.0410	.0360	.0970	.0920	.0800	.0700	.0638	.0844	.0480
CS2	.1040	.1520	.1060	.0940	.1112	.1420	.0980	.1530	.1520	.1310	.1300	.1175	.1627	.1179
CS3	.1174	.1180	.1120	.1530	.0720	.1211	.0790	.2020	.2210	.1830	.2110	.1760	.2061	.1484
PF1	.1200	.1800	.0690	.0710	.0740	.1120	.0800	.1330	.1410	.1650	.1950	.1710	.1980	.1110
PF2	.1400	.1360	.0990	.0980	.0690	.0780	.0360	.0790	.1470	.0880	.0980	.0370	.0450	.0490
PF3	.2200	.1810	.1960	.1930	.1380	.0280	.0880	.2710	.2950	.2100	.2110	.1500	.1720	.1487
PF4	.0870	.1450	.0800	.0920	.0690	.1360	.1450	.2550	.2100	.2260	.2140	.1940	.1810	.1899
PF5	.2300	.1440	.2600	.2450	.1710	.2750	.1440	.2540	.2390	.2440	.2110	.1120	.1770	.1390
PF6	.2700	.1830	.1750	.1620	.1300	.2050	.0830	.1210	.1430	.1010	.1000	.0610	.0790	.0530
PF7	.2890	.2950	.2070	.1900	.1790	.2670	.2140	.3460	.3620	.3240	.3220	.2660	.3370	.2120
PF8	.1110	.1210	.0700	.0510	.0370	.0570	.0710	.0970	.0840	.0760	.0940	.1380	.1630	.1040
PF9	.1300	.1270	.1180	.1160	.0890	.2550	.1070	.1870	.1520	.0550	.0560	.1440	.1120	.1520
PF10	.2400	.1190	.2520	.2630	.1720	.1890	.1790	.2820	.2350	.3190	.3268	.2287	.3070	.2150
AP1	.0860	.0860	.0430	.0390	.0300	.0460	.0310	.1810	.1810	.1100	.1080	.0870	.1610	.1050
AP2	.1020	.1020	.1200	.1040	.0410	.0730	.0820	.0410	.0410	.0250	.0240	.0210	.0290	.0380
AP3	.1940	.1940	.1570	.1780	.1330	.2400	.0880	.1710	.1710	.2050	.2090	.1130	.2180	.0800
AP4	.1870	.1870	.1620	.1660	.1380	.0900	.0770	.2910	.2910	.2980	.3240	.1470	.1670	.1090
AP5	.2960	.2960	.1700	.1950	.0610	.2750	.1440	.2760	.2760	.1700	.1950	.1610	.2750	.1140
AP6	.1210	.1210	.1110	.1120	.1150	.1260	.1210	.1010	.1010	.1980	.1970	.1720	.1220	.1570
AP7	.1290	.1290	.1810	.1800	.1560	.1440	.0990	.3980	.3980	.2590	.2590	.1400	.1230	.1520
AP8	.1830	.1830	.1550	.1520	.1300	.1550	.1130	.0210	.0210	.1010	.1000	.0510	.1790	.0430
AP9	.3670	.3670	.3250	.3310	.3340	.2660	.3070	.4120	.4120	.3420	.3650	.2140	.2880	.1960
AP10	.2440	.2440	.1370	.1300	.1820	.2410	.2440	.4630	.4630	.2940	.2970	.3220	.3710	.2674
AP11	.0750	.0750	.0912	.0680	.0700	.1230	.0750	.1000	.1000	.1490	.1490	.0960	.1310	.1080
AP12	.0710	.0710	.1000	.0810	.0270	.0570	.0710	.0970	.0970	.2060	.2040	.1380	.1630	.0840
AP13	.3990	.2990	.1770	.1570	.1510	.0900	.1690	.3830	.3830	.2990	.2980	.1960	.1730	.1820
AP14	.2320	.2320	.1520	.1510	.1240	.1910	.1120	.2420	.2420	.1730	.1710	.1360	.2120	.1350
AP15	.1460	.1460	.1820	.2030	.0720	.1890	.1190	.2820	.2820	.5280	.5270	.3190	.4070	.2350
AP16	.2500	.2500	.1560	.1670	.1130	.2190	.1500	.3780	.3780	.1020	.1210	.1330	.1970	.1800

**Table 7:** RMSSE after reconciliation, for all levels and methods

Series	Before COVID							After COVID						
	Base	BU	OLS	NNOLS	WLS	WLSV	MINT	Base	BU	OLS	NNOLS	WLS	WLSV	MINT
CS1	.8500	.2926	.7300	.6899	.3315	.5148	.3210	.8101	.9735	.8432	.8132	.4421	.6427	.5935
CS2	.2975	.2597	.3300	.2905	.2165	.2585	.2890	.6108	.8876	.7900	.7699	.3496	.6863	.3996
CS3	1.2340	3.2340	1.1000	1.0497	.9785	1.4216	.8110	1.8258	2.9028	2.7746	2.6442	1.0441	1.7909	1.3296
PF1	1.2514	.4825	1.1825	1.1919	.8311	.8759	.3725	1.2734	1.0944	.3565	1.3551	.4597	.9080	1.0944
PF2	.9094	.3323	.9508	.9544	.5853	.4715	.3163	.8255	.6468	.5642	.5643	.3686	.4318	.6468
PF3	1.7796	1.8292	1.7885	2.0019	1.2811	.6962	1.3796	2.5599	3.9093	2.4894	2.4858	.7114	.8537	.5480
PF4	.8804	.4432	.8115	1.6368	.7807	1.0321	.4042	2.1496	2.8502	1.7114	1.7196	1.0763	2.3910	.8502
PF5	3.2135	3.2135	1.7466	2.1832	1.7532	1.2741	1.0332	2.7705	2.0253	2.1935	2.1563	1.1665	1.8132	.7529
PF6	1.1544	.7544	1.1373	1.4343	.7931	.6726	.6347	1.5091	.8391	1.5415	1.5402	.4812	.9168	.5391
PF7	.5860	.8680	.1549	.0923	.1073	.0806	.1237	.7630	.4630	1.3916	1.0918	.4882	.6541	.4630
PF8	.4999	.9399	.1111	.1169	.0948	.1510	.0999	.8568	.5991	.5954	.6651	.5117	.7951	.4991
PF9	2.3414	1.6080	.5601	.5533	.4098	1.4517	.4802	2.4231	1.6496	2.2739	2.3967	1.2019	1.3616	1.6496
PF10	2.6340	2.4779	.9798	1.3010	1.1216	1.1588	.9013	3.7584	3.8628	2.8346	2.8464	1.0297	2.8109	1.4563
AP1	1.7226	1.7226	1.0207	1.6699	.9825	1.0449	.8226	2.4580	2.4580	2.7238	2.7099	1.2516	1.3846	1.1081
AP2	.8710	.8710	.7571	.7666	.5767	.5026	.4710	.8318	.8318	1.1283	1.1281	.4200	.6259	.4872
AP3	.7796	.7796	1.9968	1.8277	.7059	.9877	.4796	1.1590	1.1590	1.3443	1.3559	.6043	1.7601	.5480
AP4	2.5067	2.5067	2.9258	2.9010	1.4763	1.6079	1.1067	3.0681	3.0681	1.9185	2.8995	1.4595	2.8748	1.8039
AP5	3.2135	3.2135	1.7466	1.6635	1.6532	3.3697	1.2135	3.0005	3.0005	2.1935	2.1563	1.5665	2.4366	2.0253
AP6	.6460	.6460	.4012	.4044	.3365	.2560	.2460	.8516	.8516	1.5946	1.5943	.3758	.6583	.6329
AP7	1.1353	1.1353	1.5412	1.5380	1.0957	1.0255	.7353	1.2203	1.2203	1.4608	1.4615	1.2796	2.1847	1.4387
AP8	1.1544	1.1544	2.1373	2.1343	.9931	1.5479	.7544	2.5091	2.5091	2.5415	2.5402	.4812	.9168	.8391
AP9	1.1474	1.1474	2.6218	2.4743	1.3002	1.4370	.7474	2.9291	2.9291	3.0567	3.1055	.1419	2.8455	2.4862
AP10	.4702	.4702	.1554	.2553	.1567	.1692	.1002	1.8843	1.8843	1.7840	1.6847	.6024	.7727	.5308
AP11	1.1219	1.1219	1.1889	1.1927	.9676	1.8498	.7219	1.9539	1.9539	1.3540	1.3532	.3079	1.0097	.8235
AP12	.4999	.4999	.1111	.1169	.2948	.1510	.0999	1.8357	1.8357	1.7954	1.8951	.6117	.6951	.4991
AP13	1.8604	1.8604	.7458	.7446	.8582	.7142	1.4604	1.5216	1.5216	2.2831	2.2842	1.2929	2.2325	2.4452
AP14	1.9526	1.9526	1.0600	1.5021	.6333	1.0797	.5526	2.3568	2.3568	1.1362	1.1390	.7425	1.2788	.5336
AP15	3.2340	3.2340	.9798	1.5448	2.0479	1.1599	.8740	3.3258	3.3258	2.9346	2.9464	1.0297	2.4109	2.5628
AP16	1.1624	1.1624	.9668	.8633	.4236	.2642	.4624	1.7590	1.7590	1.3981	1.3792	.8790	1.3590	1.2826